P: ISSN No. 0976-8602 RNI No.UPENG/2012/42622 VOL.-V, ISSUE-II, April-2016
E: ISSN No. 2349-9443 Asian Resonance

Removal of Dye Safranin-T from Aqueous Solution by Adsorption Onto PVA/Alginate Bound Nano Magnetite Hydrogel Microspheres

Prerna Kathane
Assistant Professor,
Deptt.of Chemistry
Govt. V.Y. T. P.G.Auto College,
Durg, Chhattisgarh

Alka Tiwari
Professor,
Deptt.of Chemistry,
Govt. V.Y. T. P.G.Auto College,
Durg, Chhattisgarh

Abstract

Novel adsorbent polyvinyl alcohol-alginate bound nano magnetite hydrogel microspheres (PVA-ANM) has been synthesized and its potency for removal of dye safranin–T (ST) from aqueous solutions was examined by batch sorption technique. Effect of pH, adsorbent dose, temperature, dye concentration and contact time were investigated. Adsorbent was characterized by TEM, FTIR and XRD techniques. Adsorption data fitted well with Langmuir and Freundlich isotherm models. Adsorption process belonged to pseudo-second order kinetic model. Blend technique of ionic interaction with magnetic separation involved in removal process. Good regeneration and reusability obtained. This ecofriendly, economic adsorbent exhibited high potency for water remediation.

Keywords: Nano Magnetite, Dye Safranin-T, Polyvinyl Alcohol-Alginate, Adsorption Isotherm

Introduction

Dyestuff in waste water from numerous industries such as textiles, printings, paper, rubber, plastic, leather, cosmetic, food, pulp mill and drugs is stable and resistant to biodegradation because of its complex aromatic molecular structure.[1] . Dyes are considered as hazardous material and most of dyes are listed to be toxic, carcinogenic and mutagenic by USEPA. During dyeing process huge amount of unfixed dyes may be lost to the effluent, these exculpated into water bodies, causes deterioration in water quality, which represent an aesthetic problem and reduce photosynthetic activity and may also have a measurable impact on human health and aquatic organisms due to toxic, carcinogenic and mutagenic effects of some dyes or their metabolites.[2, 3] Thus the removal of such colored toxic dyes from wastewater has become essential. Much treatment technologies have been reported to remove dyes from wastewater including coagulation, flocculation, chemical oxidation, membrane/ultra filtration, ion exchange, photo degradation, catalysis and adsorption [4-8]. Among these technologies adsorption is a veritable alternative due to its simplicity, good selectivity, moderately high removal performance, cost effectiveness, easy generation process of adsorbents, sludge free treatment and high efficiency as well as the availability of a wide range of adsorbents. Some reported adsorbents for cationic dye removals are activated carbon, clay, biomasses, polymers, zeolites, resins, nano-materials [9-12] etc.

Safranin-T (ST) is one of the most commonly used water soluble, reddish brown colored, cationic phenazine dye, IUPAC name is 3,7-Diamino-2,8-dimethyl-5-phenylphenazinium chloride, structure is shown in Fig.-1

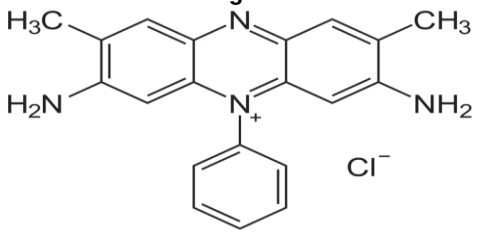

Fig. 1 Chemical structure of Safranin-T

ST is specially used as food dye in flavoring and colouring candies, cookies, histology and cytology for the detection of cartilage, mucin and mast cell granules as a biological stain that is consider to be carcinogenic in nature. Due to its vast use in textile and food industries as colorant, Safranin was designed as the model compound to express the dyes that are released in effluents from the textile and food industries. Exposure to these effluents can be irritating to respiratory systems, skin, and digestive tract infections when ingested.[13] The products formed after degradation of ST are unsafe having carcinogenic and mutagenic potential. It is therefore, crucial to decolorize waste water to the minimum permissible concentration in order to escort the water bodies as governed by environmental regulations. Various adsorbents reported for ST removal includes, thuja orientalis [13] pine sawdust [14] activated carbon [15,16] agriculture/bio-wastes [17-20] nano-materials [21-23].Unfortunately removal capacities of these adsorbents are not as good as required and prohibited large scale utilization due to engineering difficulties, such as dispersion problem, expertise and regeneration cost. Hence there is demand for an inexpensive, efficient and eco-friendly adsorbent for the removal of cationic dyes. In this regard a novel adsorbent PVA/alginate bound nano-magnetite hydrogel microsphere (PVA/ANM) has been developed for the effective removal of cationic dye ST from aqueous solution. Polyvinyl alcohol (PVA) is low cost, non toxic, biocompatible highly durable and mechanically great stable polymer. Alginate is a natural biopolymer, extracted mainly from brown seaweed (algae). PVA and alginate have been gained very importance in field of water remediation due to their biodegradability, immunogenicity and ability to form a gel with a variety of cross linking agents.[10] Mixed polymer (PVA/Alginate) exhibited rubber like elastic properties, PVA contributed strength and durability to the microspheres, where as calcium-alginate improved the surface properties reducing the tendency to agglomerate.[24] Polymer based nano and micro magnetic particles (usually magnetite nano γFe_3O_4) have been gained attention by most of researchers because it is possible to regulate their size, morphologies and design their functional groups to widespread applications in field of bioscience, chemistry and environmental remediation.[25] Basically commercially available magnetic particles are rather expensive and cannot be employed for large scale processes. Because of large surface area, great magnetic characteristics and surface energy composite PVA-ANM microspheres tend to adsorb toxic cations and competent sorption potential, holds easy and fast resolution of organic cationic dye from aqueous solution.

Objective of the Study

Objectives of present work include

1. Synthesis of PVA/alginate bound nano-magnetite hydrogel microspheres (PVA-ANM).
2. Characterization of these PVA-ANM adsorbent by TEM, XRD and FTIR techniques.
3. Batch adsorption studies of these microspheres to examine their dye ST removal capacity from aqueous solution.
4. Batch sorption kinetic and equilibrium study of the data obtained by the sorption experiments
5. Illustration of mechanism of dye ST adsorption based on the results.
6. Desorption study for recovery and regeneration of adsorbent.

Review of Literature

M. Lezehari et al. reported alginate encapsulated pillared clay was prepared and its application in removal of a neutral/anionic biocide (Pentachlorophenol) and a cationic dye (safranine) from aqueous solution [1]. I. Safarik et al. applied peanut husks magnetic fluid modified as an adsorbent for organic dye removal [2] Z. Hasan and coworker reported removal of hazardous organics from water using metal-organic frameworks: Plausible mechanisms for selective adsorbent [3] Removal of methylene blue dye from aqueous solutions by adsorption using yellow passion fruit peel as adsorbent carried out by A. Cristina et al. [4] M.T. Sulak et al reported removal of textile dyes from aqueous solutions with eco-friendly biosorbent [5]. Removal of Safranin T from wastewater using micellar enhanced ultra filtration carried out by N. Zaghbani et al. [6] L. Ai et al. investigated adsorption of methylene blue from aqueous solution with activated carbon/cobalt ferrite/alginate composite beads: kinetics, isotherms and thermodynamics [7], Removal of dyes from wastewaters by adsorption on pillared clays has been reported by A. Gil and coworker [8]. M. Yusuf et al. attempted kinetic studies of Safranin-O removal from Aqueous Solutions using Pineapple Peels and found that system closely followed second order kinetics [9] Sorption kinetics for the removal of dyes from effluents onto chitosan has been conducted by Y. C. Wong et al. [10] S. Bayazit reported investigation of safranin-O adsorption on super paramagnetic iron oxide nanoparticles (SPION) and multi-wall carbon nanotube /SPION composites [11] Decolorization of the aqueous safranin O dye solution using thuja orientalis as biosorbent has been reported by D.E. Al-Mammar et al. [12] V.K., Gupta et al. carried out adsorption of safranine-T from waste water using waste materials activated carbon and activated rice husk [13] S. Preethi et al. attempted removal of safranin basic dye from aqueous solutions by adsorption onto corncob activated carbon[14] Linear and nonlinear regression analyses for binary sorption kinetics of methylene blue and safranin onto pretreated rice husk has been reported by S. Chowdhury et al. [15] M.A. Mohammed Ibrahim et al. attempted batch removal of hazardous safranin-O in wastewater using pineapple peels as an agricultural waste based adsorbent [16] M. R. Malekbala and coworker investigated equilibrium and kinetic studies of safranine adsorption on alkali-treated mango seed integuments [17] A. Soni et al. attempted removal of malachite green from aqueous solution using nano-iron oxide-loaded alginate microspheres: batch and column studies, [18] Alginate/PVA-Kaoline composite

for removal of Methylene blue from aqueous solutionshas been carried out by M.M Abe El-Latif et al. [19] B.H Hameed et al reported malachite green adsorption by rattan sawdust: Isotherm, kinetic and mechanism modeling, [20] L. Wang et al attempted adsorption of basic dyes on activated carbon prepared from polygonum orientale linn: equilibrium, kinetic and thermodynamic studies [21]

Material and Method

Materials

The polyvinyl alcohol, sodium alginate, sodium hydroxide pellets, calcium chloride and ammonium hydroxide were purchased from Loba-Chemie, Mumbai, India, anhydrous ferric chloride and ferrous chloride tetrahydrate were purchased from Molychem, Mumbai, India. Triple distilled water was used throughout the experiments.

Synthesis of PVA-ANM Microspheres

Adsorbent PVA-ANM hydrogel microsphere was synthesized according to the following steps:-

First step involves preparation of viscous gel of polyvinyl alcohol (PVA) by dissolving at 90^{o}C in hot triple distilled water and was mixed thoroughly with the viscous gel of sodium alginate to get 1:1 ratio, stirred for 2 h for homogeneity and kept aside to obtain a bubble free solution.

In second step the microspheres were prepared by drop wise addition of the above mixture in $CaCl_2$ solution (0.5M) for cross linking. The microspheres so produced were allowed to harden by leaving them in solution for 24 h then washed several times with distilled water.

In the third step for in-situ magnetization, these microspheres were equilibrated in an aqueous solution of ferrous chloride tetrahydrate and ferric chloride in 1:3 ratios for 24 h.

In the fourth step the microspheres were then added into alkaline solution and kept for 2 h, so that the Fe^{2+}/Fe^{3+} ions get precipitated into iron-oxide within the PVA-Alginate matrix. These PVA-ANM hydrogel microspheres were then thoroughly washed several times and stored for adsorption studies.

Fig. 2 Photograph showing PVA-ANM hydrogel microspheres

Batch Adsorption Experiments

Stock solution of dye ST of 1000 mg/L was prepared by dissolving 1.000g of dye safranin-T in 1000 mL triple distilled water. Suitable concentrations of dye safranin-T for batch experiments were prepared by diluting the stock solution with triple distilled water. Fresh dilutions were used in each experiment.

Adsorption experiments were accomplished by differing pH, agitation time, dose of adsorbent, initial concentration and temperature. For sorption experiments PVA-ANM microspheres 0.2 g and 20 mL dye ST solution of 10 mg/L concentration at pH 10 and room temperature (25℃ ±2) was agitated in an orbital shaking machine at 200 rpm for 150 min, which was found to be a sufficient speed and time to attain equilibrium adsorption. The amount of dye ST present in solution (before and after equilibrium adsorption) was examined by UV-Visible spectrophotometer (Systronic-117). The removal percentage and removal capability of adsorbent was calculated by the equations 1 and 2, respectively as given below:

$$Removal\ percentage = \frac{C_i - C_e}{C_i} \times 100\% \quad (1)$$

$$Removal\ capability = C_i - C_e \times \frac{V}{m} \quad (2)$$

where C_i and C_e are the initial and equilibrium concentration mg/L) of dye ST respectively, V (L) is the volume of the adsorbate solution, subjected to sorption and m (g) is the weight of adsorbent.

Desorption Studies

Desorption Studies confirms the nature of sorption and recovery of adsorbate from adsorbent in aqueous medium. After adsorption experiments, the dye loaded adsorbent (ST adsorbed PVA-ANM) was collected by filtration and treated with nitric acid of distinct strength ranging from 0.05 to 0.3 M. Desorption efficiency was calculated by using following equation:-

$$Desorption\ \% = \frac{Amount\ \ of\ dye\ \ desorbed}{Amount\ \ of\ dye\ \ adsorbed} \times 100 \quad (3)$$

Characterization of PVA-ANM adsorbent

The Transmission Electron Microscopy (TEM) Analysis

TEM Analysis was carried out to observe the average particle size, distribution of particles and morphology of nano magnetite iron-oxide particles by TECNAI-G-20 transmission electron microscopy (TEM) at a voltage of 200 kV.

X- Ray Diffractometer (XRD) Analysis

Crystalline nature of PVA-ANM were examined on a Brucker D8 advanced XR Diffractometer with scanning range of 20^{o}-80^{o} (2θ) using Cu_Ka radiation with wavelength of 1.5406A^{o}.

Fourier Transform Infrared (FTIR) Analysis

FTIR spectra of PVA-ANM adsorbent bare and cationic dye loaded were measured using Varian Vertex FTIR spectrometer.

Results and Discussion

Characterization of PVA-ANM adsorbent

TEM analysis

TEM Image denoted almost cubic iron-oxide particles with an average particle size < 10 nm. It should be pointed, although, that the majority of particles were scattered, a few of them showing aggregates indicative of stabilization of nano-magnetite particles, as shown in Fig 3, TEM images revealed that the size of individual nanoparticles seems to be 3-9 nm.

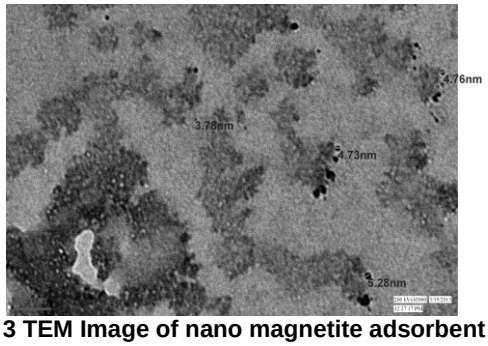

Fig. 3 TEM Image of nano magnetite adsorbent

XRD analysis

XRD pattern of adsorbent PVA-ANM is shown in Fig. 4, it has revealed five characteristics peaks. The position and relative intensities of all diffraction peaks are match well with those from the JCPDS file number 89-5984 for magnetite ($\gamma Fe_3 0_4$). The diffraction peaks at 2θ angles appeared in order of 26.93°, 31.89°, 38.87°, 41.23° and 45.55° can be marked by their scattering from (101), (110), (112), (114), (119) and (200) plane of the adsorbent's powder type crystal lattice, respectively. Magnetite particles are obtained according to the following reaction:

$$2FeCl_3 + FeCl_2 + 8NH_4OH \longrightarrow Fe_3O_4 + 8NH_4Cl + 4H_20$$

Average crystallite size of as prepared nano magnetite adsorbent is obtained 36.89 nm.

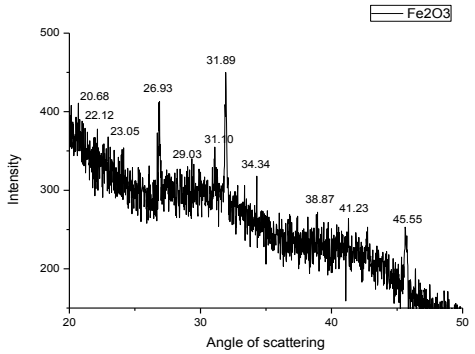

Fig. 4 XRD pattern of adsorbent nano magnetite PVA-Alginate matrix

FTIR analysis

FTIR is an important tool to identify the functional groups present on an adsorbent. The vibrancy signals of PVA-ANM microspheres before (i) and after adsorption of dye safranin-T (ii) were different, as shown in Fig 5. By comparing the spectra of magnetite microspheres before and after safranin-T adsorption, the following conclusions could be drawn. The shifting of –OH stretching band from 3380 to 3406 cm^{-1} suggests the attachment of adsorbate dye ST. The shifting of the C-O band to the higher frequency from 1425 to 1417 cm^{-1} can be attributed to the association of the hydroxyl group with adsorbate cationic dye. The shifting of the C-O band to the higher frequency from 1027 to 1034 cm^{-1} can be attributed to the association of the oxalate group with adsorbate. The characteristic peak at 465 cm^{-1} relates to Fe-O group, which indicates the loading of nano iron-oxide particles on cross-linked PVA-Alginate matrix.[26] A slight shift of Fe-O band from 465 to 479 cm^{-1} shows the adsorption of some of the adsorbate dye ST onto the nano magnetite iron-oxide surface.

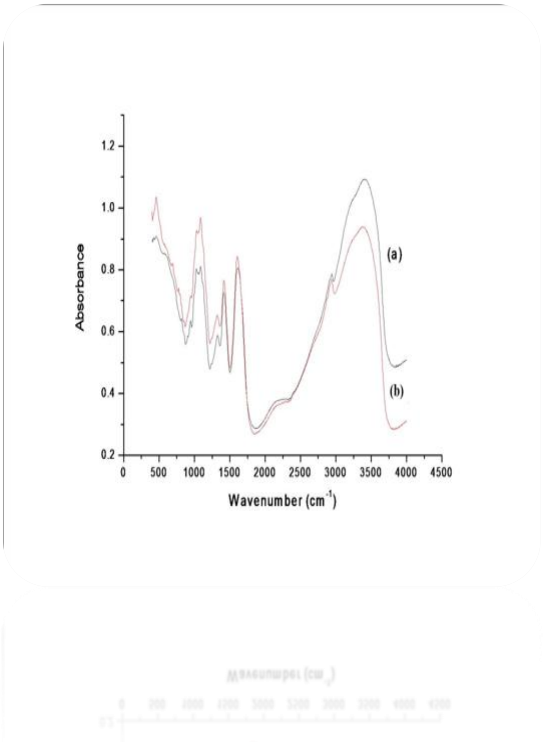

Fig. 5 FTIR spectra of PVA-ANM hydrogel microspheres before (a) and after adsorption (b) of dye ST

Adsorption Isotherm Models

The adsorption isotherms describe how adsorbed molecules are dispersed between liquid phase and solid phase when equilibrium reaches in adsorption process. Adsorption isotherms study was applied to investigate the sorption capability of adsorbent using most widely accepted isotherm models namely Langmuir and Freundlich.

Langmuir isotherm model

Langmuir isotherm is based on the assumption that adsorption energy is constant as well

as independent of surface coverage and maximum adsorption occurs when the surface is covered by monolayer of adsorbate.[27] The linearized Langmuir adsorption isotherm is given by Eq. 4.

$$\frac{C_{eq}}{q_{eq}} = \frac{1}{K_a q_{max}} + \frac{C_{eq}}{q_{max}} \qquad (4)$$

where C_{eq} is the equilibrium concentration of solute in bulk solution (mg/L), q_{eq} is amount of solute adsorbed per unit weight of adsorbent (mg/g), K_a is sorption equilibrium constant and q_{max} represent adsorption capacity (mg/g). The values of q_{max} and K_a can be calculated from the slope and intercept of the plot C_{eq} versus C_{eq}/q_{eq}, originated a linear graphical relationship indicating application of the above model as shown in Fig. 6 (a). Values are given in Table-1.

An essential characteristics of Langmuir equation is separation factor R_L used to evaluate the feasibility of adsorption to adsorbent, can be calculated by Eq. 5.

$$R_L = \frac{1}{1+K_a C_i} \quad (5)$$

where C_i is the initial dye concentration(mg/L) and K_a is Langmuir constant(L/mg). Value of R_L indicates the type of isotherm to be either unfavorable (R_L>1), linear (R_L= 1), favorable (0<R_L<1) or irreversible (R_L= 0). The R_L value was observed between 0 and 1, showing favorable adsorption of dye ST onto PVA-ANM microspheres.[28,29]

Freundlich isotherm model

Freundlich isotherm presumes that the adsorption of organic dyes occurs on a heterogeneous and the multilayer surface of varied affinities. Logarithmic form of Freundlich equation is as follows.

$$log q_{eq} = log K_F + \frac{1}{n} log C_{eq} \quad (6)$$

where q_{eq} is the adsorbed amount of dye ST at equilibrium (mg/g), K_F and n are the Freundlich constants related to adsorption capacity and adsorption intensity; respectively. A plot of $log\ q_{eq}$ versus $logC_{eq}$ gives a straight line as depicted in Fig. 6 (b). The calculated adsorption intensity n is 2.105, which indicated favorable adsorption. In general n>1 suggests satisfactorily adsorption higher n value means stronger sorption intensity. Values are given in Table 1.

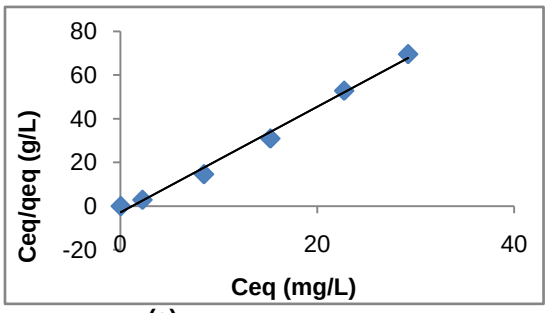

(a)

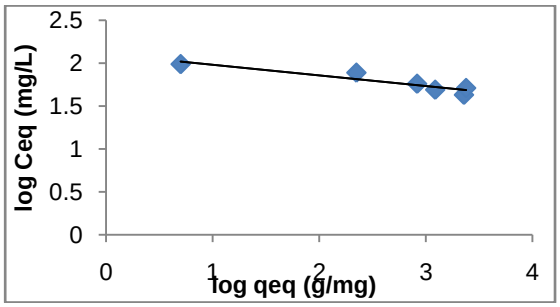

(b)

Fig. 6 Langmuir adsorption isotherm (a) and Freundlich adsorption isotherm (b) of dye ST adsorption onto PVA-ANM hydrogel microspheres

Table 1 Results of Isotherm Parameters for dye ST adsorption onto PVA-ANM hydrogel microspheres at 25℃

S. No.	Isotherm Model	Parameters	R^2
1.	Langmuir Isotherm	K_a = 0.334 L/mg q_{max} = 98.71 mg/g R_L = 0.0565 to 0.2304	0.992
2.	Freundlich Isotherm	K_F = 8.76 L/mg N = 2.105	0.870

Adsorption Kinetic Studies

Adsorption kinetic studies are important in specifying the sorption rate and mechanism which in turn regulates the residence time of adsorbate at the solid-liquid interface and also provides valuable insights information of reactions pathway. The improvement of the adsorption process was governed at different time intervals (0-240 min), which clearly exhibited that sorption of cationic dye ST increased with the increase in time and then flatten out after 150 min.

Pseudo-first order kinetic model

Lagergren suggested a pseudo-first order kinetic model. The integral form of model is given by the Eq. 7.

$$\log(q_e - q_t) = log q_e - \frac{K_{ad}}{(2.303)} t \quad (7)$$

where q_e and q_t are the adsorption capability (mg/g) at any time (t) and at equilibrium, respectively. K_{ad} is the pseudo-first orders rate constant of sorption. K_{ad} and the correlation coefficient for dye ST adsorption were evaluated from the linear plot of $log(q_e - q_t)$ versus t as shown in Fig. 7(a), the values are given in Table 2. The correlation coefficient for pseudo-first orders is low. Besides a large variance in equilibrium adsorption capability (q_e) between experiment and calculation was observed, indicating a poor pseudo-first order fit to the experimental data.

Pseudo-second order kinetic model

Ho McKay has been suggested a pseudo-second order kinetic model for adsorption. The linearized integral form of the model is expressed by Eq. 8.

$$\frac{t}{q_t} = \frac{1}{k_2 q_t^2} + \frac{1}{q_e} t \quad (8)$$

where k_2 q_t^2= h (mg/g. min) can be observed as the initial dye adsorption rate when t→0 and k_2 is the rate constant of the pseudo-second order equation. The plot of t/q_t versus t may give a straight line, as shown in Fig. 7(b). q_e and h can be determined from slope and intercept of plot, respectively, at initial dye

concentration (10 mg/L) a straight line with very high correlation coefficient (0.999) was achieved, values are given in Table 2. In essential, the evaluated q_e value also agrees with the experimental data in case of pseudo-second order kinetics. This advocates the assumption that rate-determining step of dye ST adsorption on the adsorbent may be chemisorption. In chemisorption, cations of dye attach to the adsorbent surface by forming a chemical bond (mostly covalent) and lead to asset sites that maximize their coordination number with the surface.[20-21]

Intraparticle diffusion

The kinetics of adsorption of a adsorbate onto adsorbent may be governed by three dynamisms, viz. film diffusion, pore diffusion and intraparticle transport. Most probably pore diffusion is rate controlling step in batch adsorption process. A plot was drawn between amounts of adsorbed dye ST on adsorbent qt versus t1/2, to evaluate the rate-limiting step as depicted in Fig 8. The rate constant for intraparticle diffusion was determined from the slope of the linear portion of curve by Morris-Weber Eq. 9.

qt=Kpt1/2+C (9)

where Kp (g/mg. min−1/2) is rate constant for intraparticle diffusion, C gave information about the thickness of outermost layer. Adsorption mechanism follows the intraparticle diffusion process, which proves the physical phenomenon impact; values are giveninTable2.

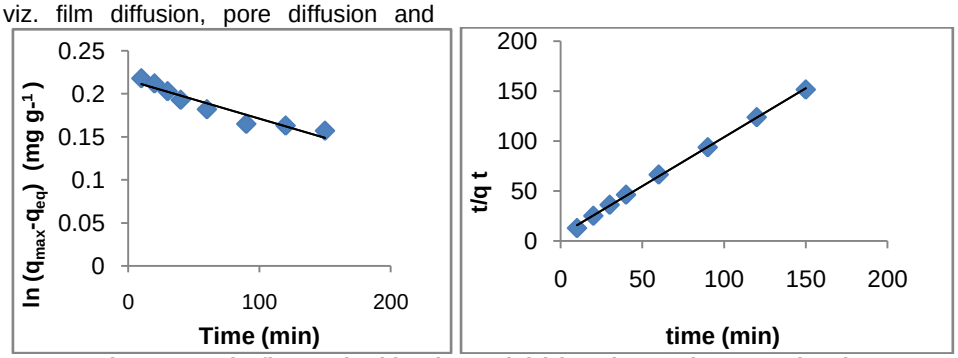

Fig. 7 Pseudo-first order kinetic model (a) and Pseudo-second order kinetic model (b) for dye ST sorption onto PVA-ANM hydrogel microspheres

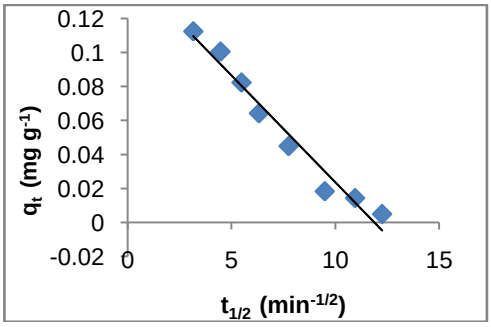

Fig. 8 Intraparticle diffusion plot of dye ST adsorption by PVA-ANM microspheres

Table 2 Results of Kinetic parameters for dye ST adsorption by PVA-ANM hydrogel microspheres at 25℃

S.No.	Kineticsmos	Parameters	R^2
1.	Pseudo-first order	K_{ad} = 0.0936 min^1 q_{max} = 98.67 mg/g	0.916
2.	Pseudosecond order	k'_2 = 0.170 g/mg. min q_{max} = 98.00 mg/g h =0.1734 mg/g. min	0.999
3.	Intraparticle diffusion	Kp = 0.012 mg/ $min^{1/2}$	0.967

Mechanism of Dye ST adsorption onto PVA-ANM Adsorbent

Surface characteristics of an adsorbent plays a vital role in dye sorption potency which may also affected by the initial pH of solution. Basic pollutants may be expected to have larger affinity to negative groups of adsorbent at basic pH (ionic interaction).[3, 24] The most suitable sorption mechanism of uptake of dye ST onto PVA-ANM is illustrated in Fig 9.

1. FTIR analysis revealed that the heterogeneous surface of nano magnetite cross-linked PVA/alginate matrix contains electron rich groups viz. oxalate (--O^-), carboxylate (---COO^-) and hydroxyl (--OH^-).
2. Cationic dye ST coordinate with these anionic carboxylate (a), hydroxyl (b) and oxalate (c) groups of adsorbent by electrostatic interactions, respectively.
3. In augmentation, cationic dye ST may also co-ordinate with electron rich oxygen of nano magnetite iron-oxide (γFe_3O_4) particles within PVA/Alginate co-polymeric matrix of hydrogel microspheres (d).

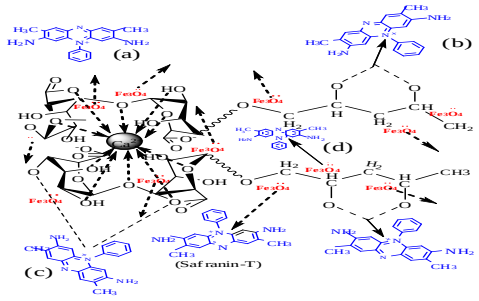

Fig. 9 Mechanism of dye ST uptake onto PVA-ANM hydrogel microspheres

Factor affecting the sorption

Effect of pH

The pH value is an important factor which can determine surface charge on adsorbent and ionization degree of adsorbate. Experiments were conducted at pH ranged from 2 to 12, as shown in Fig. 10 (a). Maximum removal was obtained at pH 10 (> 98%). At low pH, the decrease in adsorption may be attributed by two reasons. Firstly the number of positively charged surface sites increased, due to electrostatic repulsion. Secondly the availability of excess H^+ ions competing with dye cations for the adsorption sites present on adsorbent. At higher pH, the surface of PVA-ANM sorbent may get negatively charged groups which enhance significant enlargement of cationic dye ST uptake.

Effect of adsorbent dosage

The adsorption of ST onto PVA-ANM microspheres was studied at 25°C by varying the adsorbent dose from 0.05 to 0.3 g while keeping all other parameters (pH, time and concentration) constant, as shown in Fig.10 (b). The percentage adsorption was noticed to increase with the increase in adsorbent dose from 0.05 to 0.2g which may be due to increased surface area and availability of more adsorption sites.

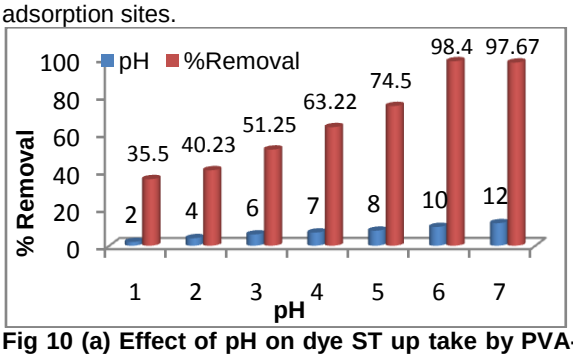

Fig 10 (a) Effect of pH on dye ST up take by PVA-ANM hydrogel microspheres

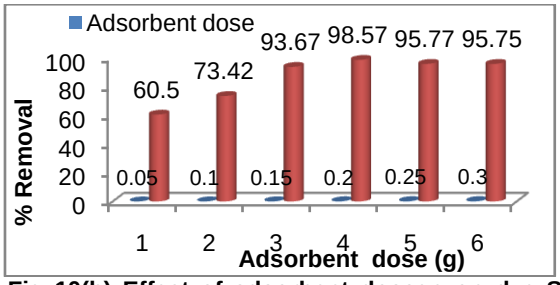

Fig 10(b) Effect of adsorbent dosage on dye ST uptake by PVA-ANM hydrogel microspheres

Effect of concentration

Sorption kinetics is especially depends on concentration of cations solution. The effect on adsorption experiments of dye ST concentration in the range of 01 to 50 mg/L were examined in order to understand the adsorbate and adsorbent interaction. It is evident from Fig. 10(c) that dye uptake increased with increasing concentration of dye ST solution and the maximum removal was found at 10 mg/L. Above this concentration, a decrease in the adsorbed amount was noticed which may be due to progressive saturation of binding sites.

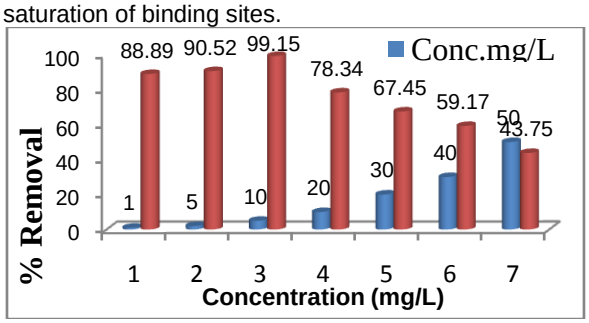

Fig 10(c) Effect of concentration on dye ST uptake by PVA-ANM hydrogel microspheres

Effect of agitation time

Agitation time is one of the important factors in adsorption process. Removal of dye ST was studied as a function of agitation time in the range between 10 to 180 min. Uptake of dye increased with increasing contact time and became approximately constant after 150 min, as shown in Fig. 10(d). Initially rate of adsorption is higher because a greater surface range of adsorbent is feasible for cationic dye uptake, however decreased to a constant value with increase in contact time because of all available sites was covered and no active site available for binding.

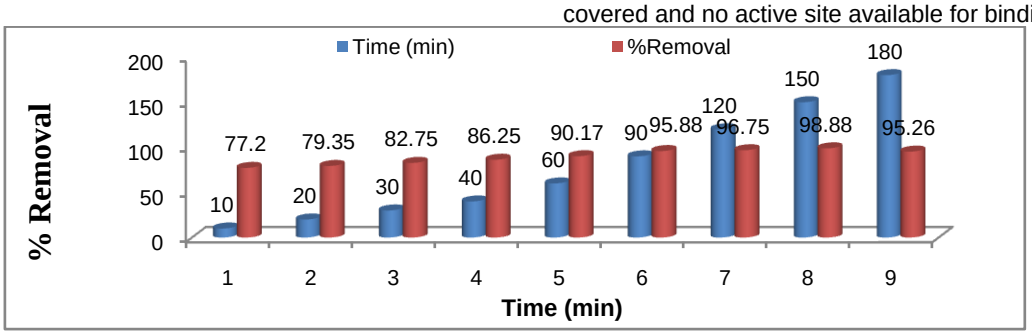

Fig 10 (d) Effect of time on dye ST up take by PVA-ANM hydrogel microspheres

Effect of Temperature

Experiments were conducted at temperature 15, 25, 35, 45 and 55℃ while keeping all other parameters (pH, time and concentration) constant. Maximum removal achieved at 25℃, when temperature was increased from 25 to 55℃

adsorption decreased from 98.75 to 61.38%, as shown in Fig 10(e) due to molecules move with great speed and less time of interaction was available for dye cations with active site of adsorbent material. Increase viscosity also enhanced diffusion rate of adsorbate across external boundary layer and internal pores of the adsorbent.

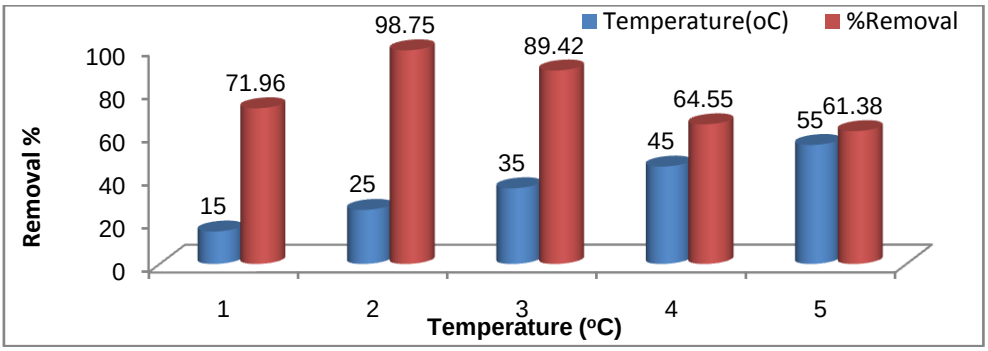

Fig 10 (e) Effect of Temperature on dye ST Up Take by PVA-ANM hydrogel Microspheres

Desorption and Regeneration Study

It is essential to investigate the reusability of adsorbents for realistic applications to govern ecological and economic needs for sustainability. The cationic dye ST loaded adsorbent microspheres were collected, washed and then treated with various desorbing agents namely nitric acid, hydrochloric acid, acetic acid, sodium hydroxide and sodium chloride solutions, the nitric acid has been found a more competent than others. > 99% desorption of dye ST from the adsorbent obtained with 0.1 M HNO3 acid at 25℃. Composite nano magnetite co-polymeric adsorbent revealed relatively the equivalent dye uptake capability after consecutive regeneration. In acidic medium, protons conflict with dye and expel the utmost bulk of adsorbed dye. Thus ion exchange kinetics is relevant with reference to adsorption/desorption process for used adsorbent.

Conclusions

PVA-ANM hydrogel microspheres have been synthesized by insitu magnetization and assessed its sorption efficiency for removal of cationic dye ST by batch sorption technique. Maximum removal of dye ≥ 98% was noticed at pH 10 and 25^0C in 150 minutes, which was higher than that of most of the traditional adsorbent. Sorption isotherm follows Langmuir model better than Freundlich isotherm model. The kinetic data closely followed pseudo second order rate model. PVA-ANM has been found to be very effective, efficient, ecofriendly and economic adsorbent for the removal of cationic dyes from water. The investigated technique proves great potential for up taking the cationic dye with high percentage removal and also exhibited its efficiency in multiple cycles of usage. Blend technique of adsorption with magnetic separation involves expedient resilience, ecofriendly property. Recovery of adsorbent and adsorbate is beneficial and exciting. FTIR results of nano-magnetite adsorbent showed various functional groups which were identified as potential adsorption sites responsible for binding ST. It is expected that reported adsorbent PVA-ANM could be of great potential as a new grade of adsorbent for cationic toxic dye elimination from aqueous solution and explicit expedient in the field of water remediation.

Acknowledgments

The authors are thankful to UGC-DEA consortium of Scientific Research Centre, Indore, India for FTIR & XRD and AIIMS New Delhi, India for TEM analysis.

References

1. Lezehari M., Basley J.P., Bouraso B.M. (2010), Alginate encapsulated pillared clay: Removal of a neutral/anionic biocide (Pentachlorophenol) and a cationic dye (safranine) from aqueous solution, Colloids Surf. A, Vol. 366, pp 88-94.
2. Safarik I. and Safarikova S.M., (2010), Peanut husks magnetic fluid modified as an adsorbent for organic dye removal, Science Direct Physics Procedia, Vol. 9, pp 274-278.
3. Hasan Z. and Jhung S.H., (2015), Removal of hazardous organics from water using metal-organic frameworks: Plausible mechanisms for selective adsorbent, J. of Hazard. Mater., Vol. 83, pp 329-339.
4. Cristina A. and Gushikem Y., (2008), Removal of methylene blue dye from aqueous solutions by adsorption using yellow passion fruit peel as adsorbent, Bioresour. Technol.,Vol. 99, pp 3162-3165.
5. Sulak M.T. and Yatmaz H.C., (2012), Removal of textile dyes from aqueous solutions with eco-friendly biosorbent, Desalination & Water Treatment, Vol. 37, pp 169-177.
6. Zaghbani N., Hafiane A., Dhahbi M., (2008), Removal of Safranin T from wastewater using micellar enhanced ultra filtration, Desalination, Vol. 222, pp 348-356.
7. Ai L., Li M., Li L., (2011), Adsorption of Methylene blue from aqueous solution with activated carbon/cobalt ferrite/alginate composite beads: kinetics, isotherms and thermodynamics, J. Chem. Eng. Data, Vol. 56, pp 3475–3483.
8. Gil A., Assis F. C. C., Albeniz S., and Korili S. A., (2011), Removal of dyes from wastewaters by adsorption on pillared clays, Chem. Eng. J., Vol. 168, pp 1032-1040.

9. Yusuf M., Elfghi F.M., Mallak S. K., (2015), Kinetic studies of Safranin-O removal from Aqueous Solutions using Pineapple Peels, Iranica J. of Energy and Environment, Vol. 6, No. 3, pp 173-180.
10. Wong Y. C., Szeto Y.S., Cheung W.H., Mckay G., (2008), Sorption kinetics for the removal of dyes from effluents onto chitosan, J. Appl. Polym. Sci., Vol. 109, pp 2232-2242.
11. Bayazit S., (2013), Investigation of Safranin-O adsorption on superparamagnetic iron oxide nanoparticles (SPION) and multi-wall carbon nanotube /SPION composites, Desalination & Water Treatment, Vol. 222, pp 1-10.
12. Al-Mammar D.E., (2014), Decolorization of the aqueous Safranin O dye solution using Thuja orientalis as biosorbent, Iraqi Journal of Science, Vol. 55(3A), pp 886-898.
13. Gupta V.K., Mittal A., Jain R., Mathur M., Sikarwar S., (2006), Adsorption of Safranine-T from waste water using waste materials activated carbon and activated rice husk, J. of colloid and interface Sci., Vol. 303, pp 80-81.
14. Preethi S., Sivasamy A., Sivanesan S., Ramamurthi V., Swaminathan G., (2006), Removal of Safranin Basic Dye from Aqueous Solutions by Adsorption onto Corncob Activated Carbon, Ind. Eng. Chem. Res., Vol. 45, No. 22, pp 7627-7632.
15. Chowdhury S.,Das P.,(2011),Linear and Nonlinear Regression Analyses for Binary Sorption Kinetics of Methylene Blue and Safranin onto Pretreated Rice Husk, Bioremediat. J., Vol. 15, pp 99-108.
16. Mohammed M.A., Ibrahim A., Shitu A., (2014), Batch removal of hazardous safranin-O in wastewater using pineapple peels as an agricultural waste based adsorbent, Int. J. of Environ. Monitoring and Analysis, Vol. 2, No. 3, pp 128-133.
17. Malekbala M. R., Soltani S. M., Yazdi S. K., Hosseini S., (2012), Equilibrium and Kinetic Studies of Safranine Adsorption on Alkali-Treated Mango Seed Integuments, Int. J. Chem. Eng. Appl., Vol. 3, pp160-166.
18. Soni A., Tiwari A. Bajpai A. K., (2013), Removal of malachite green from aqueous solution using nano-iron oxide-loaded alginate microspheres: batch and column studies, Research on Chem. Interm., 4(9), (2014) 88.
19. Abe El-Latif M.M., Elkady M.F., Ossman M.E., (2010), Alginate/PVA-Kaoline composite for removal of Methylene blue from aqus. Soln., J. of American Sci., Vol. 6, No. 5, pp 280-292.
20. Hameed B.H., El-Khairy M.I., (2008), Malachite green adsorption by rattan sawdust: Isotherm, kinetic and mechanism modeling, J. Hazard. Mater. Vol. 154, pp 237–244.
21. Wang L., Zhang J., Zhao R., Li C. Zhang C., (2010), Adsorption of basic dyes on activated carbon prepared from Polygonum orientale Linn: Equilibrium, kinetic and thermodynamic studies, Desalination, Vol. 254, pp 68-74.
22. Chaturvedi N., Sharma S., Sharma M.K., Chaturvedi R.K., (2011), Photocatalytic degradation of safranine-O in presence of nickel oxide, Int. J. of Research in chem. & Envt., Vol.1, No. 1, pp 66-70.
23. 13] Al-Mammar D.E., (2014), Decolorization of the aqueous Safranin O dye solution using Thuja orientalis as biosorbent, Iraqi Journal of Science, Vol. 55(3A), pp 886-898.
24. [14] Ozacar M., Engil A., (2005), Adsorption of metal complex dyes from aqueous solutions by pine sawdust, Bioresour. Techno, Vol. 96, pp 791-795.
25. Haider S., Binagag F.F., Haider A., Mahmood A., Shah N., Al-Masrya W. A., Ud-Din Khan S., Ramaya S.M., (2015), Adsorption kinetic and isotherm of methylene blue, safranin T and rhodamine B onto electrospunethylenediamine-grafted-polyacrylonitrile nanofibers membrane, Desalination and Water Treatment**,** Vol. 55, pp 1609-1619.
26. Soni A., Tiwari A. Bajpai A. K., (2013), Removal of malachite green from aqueous solution using nano-iron oxide-loaded alginate microspheres: batch and column studies, Res Chem. Intermed DOI 10.1007/s11164-012-1011-1.
27. Fan J., Guo Y., Wang J., Fan M., (2009), Rapid decolorization of azo dye methyl orange in aqs. soln. by nanoscale zero valent iron particles, J. Hazard. Mater. Vol. 166, pp 904-910.
28. Abe El-Latif M.M., Elkady M.F., Ossman M.E., (2010),Alginate/PVA-Kaoline composite for removal of Methylene blue from aqus. Soln., J. of American Sci., Vol. 6, No. 5, pp 280-292.
29. Xu P., Zeng G. M., Huang D. L., Feng C. L., Hu S., Zhao M. H., Lai C., Wei Z., Huang C., Xie G. X., Liu Z. F., (2012), Use of iron oxide nano-materials in wastewater treatment: A review, Sci. of the Total Environ., Vol. 424, pp 1–10.